

lial) proteins will exhibit distinctly different distance-decay properties (19).

Two key elements determine the distance dependence of electronic coupling in proteins: the directness of the coupling pathway and the energy of the tunneling electron. The former depends on the protein structure and the positions of the redox sites. In the tunneling-pathway model, the tunneling energy defines the covalent-bond coupling decay (ϵ_C); the value of 0.6 derives from analyses of ET rates in model systems (6). Changes in ϵ_C will not affect σ_i/R_M correlations, because ϵ_C appears as a prefactor in the expressions for hydrogen-bond and space-gap coupling decays. The magnitude of ϵ_C does, however, determine the predicted slopes in plots of $\log k_{\max}$ versus distance. The close agreement between the observed and predicted decay constants for azurin and cyt c suggests an ϵ_C value of 0.6 is appropriate for a high-potential oxidant such as $\text{Ru}(\text{bpy})_2(\text{im})(\text{His}^X)^{3+}$ (potential $E^0 = 1.0$ V versus the normal hydrogen electrode). In the systems analyzed by Dutton and co-workers (19), the redox couples spanned a fairly wide range, but they included many low-potential oxidants. Considering the generally less favorable tunneling energies, the reported protein decay constant [1.4 \AA^{-1} (4)] accords remarkably closely with the decay [1.26 \AA^{-1} (9)] predicted for coupling through an α -helical structure.

REFERENCES AND NOTES

- H. Sigel and A. Sigel, Eds., *Metal Ions in Biological Systems* (Dekker, New York, 1991), vol. 27; I. Bertini, H. B. Gray, S. J. Lippard, J. S. Valentine, Eds., *Bioinorganic Chemistry* (University Science Books, Mill Valley, CA, 1994).
- R. A. Marcus and N. Sutin, *Biochim. Biophys. Acta* **811**, 265 (1985).
- J. J. Hopfield, *Proc. Natl. Acad. Sci. U. S. A.* **71**, 3640 (1974); J. Jortner, *J. Chem. Phys.* **64**, 4860 (1976).
- C. C. Moser, J. M. Keske, K. Warncke, R. S. Farid, P. L. Dutton, *Nature* **355**, 796 (1992); R. S. Farid, C. C. Moser, P. L. Dutton, *Curr. Opin. Struct. Biol.* **3**, 225 (1993).
- R. A. Friesner, *Structure* **2**, 339 (1994).
- J. N. Onuchic and D. N. Beratan, *J. Chem. Phys.* **92**, 722 (1990); J. N. Onuchic, P. C. P. Andrade, D. N. Beratan, *ibid.* **95**, 1131 (1991); J. N. Onuchic, D. N. Beratan, J. R. Winkler, H. B. Gray, *Annu. Rev. Biophys. Biomol. Struct.* **21**, 349 (1992); S. S. Skourtis, J. J. Regan, J. N. Onuchic, *J. Phys. Chem.* **98**, 3379 (1994).
- P. Siddarth and R. A. Marcus, *J. Phys. Chem.* **94**, 8430 (1990); *ibid.*, p. 2985; *ibid.* **96**, 3213 (1992); *ibid.* **97**, 2400 (1993); *ibid.*, p. 13078; A. A. Stuchebrukhov and R. A. Marcus, *ibid.* **99**, 7581 (1995); J. M. Gruschus and A. Kuki, *ibid.* **97**, 5581 (1993); A. Broo and S. Larsson, *ibid.* **95**, 4925 (1991); H. E. M. Christensen, L. S. Conrad, K. V. Mikkelsen, J. Ulstrup, *ibid.* **96**, 4451 (1992); J. W. Evenson and M. Karplus, *Science* **262**, 1247 (1993); O. Farver and I. Pecht, *J. Am. Chem. Soc.* **114**, 5764 (1992).
- D. R. Casimiro *et al.*, *J. Am. Chem. Soc.*, **115**, 1485 (1993); D. R. Casimiro, J. H. Richards, J. R. Winkler, H. B. Gray, *J. Phys. Chem.* **97**, 13073 (1993); D. S. Wuttke, M. J. Bjerrum, J. R. Winkler, H. B. Gray, *Science* **256**, 1007 (1992).
- The 1.26 \AA^{-1} decay is for hydrogen bond-mediated coupling, which is much more efficient than coupling through the α -helical backbone (2.0 \AA^{-1}).
- I.-J. Chang, H. B. Gray, J. R. Winkler, *J. Am. Chem. Soc.* **113**, 7056 (1991).
- E. T. Adman and L. H. Jensen, *Isr. J. Chem.* **21**, 8 (1981).
- We expressed the proteins in *Escherichia coli* using a T7 polymerase expression system [F. W. Studier, A. H. Rosenberg, J. J. Dunn, J. W. Dubendorf, *Methods in Enzymology* (Academic Press, San Diego, CA, 1990)] and purified by fast protein liquid chromatography (FPLC) according to previously published protocols [T. K. Chang *et al.*, *Proc. Natl. Acad. Sci. U. S. A.* **88**, 1325 (1991)]. The purified proteins were incubated with $\text{Ru}(\text{bpy})_2(\text{CO})_3$ and purified again by FPLC. The addition of excess imidazole afforded $\text{Ru}(\text{bpy})_2(\text{im})(\text{His}^X)$ -azurin (10).
- We measured rates of $\text{Cu}^+ \rightarrow \text{Ru}^{3+}$ ET using a previously described technique (10). The $^*\text{Ru}(\text{bpy})_2(\text{im})(\text{His}^X)^{2+} \cdot \text{Cu}^+$ -azurin, generated by means of a 480-nm, 25-ns laser pulse, was oxidatively quenched by 5 mM $\text{Ru}(\text{NH}_3)_6^{3+}$ to yield $\text{Ru}(\text{bpy})_2(\text{im})(\text{His}^X)^{3+} \cdot \text{Cu}^+$ -azurin. Subsequent $\text{Cu}^+ \rightarrow \text{Ru}^{3+}$ ET was monitored by transient absorption at 625, 500, 432, and 310 nm. The slow ET rate in the His^{126} derivative led to a number of complications. With $\text{Ru}(\text{NH}_3)_6^{3+}$ as a quencher, $\text{Cu}^+ \rightarrow \text{Ru}^{3+}$ ET was in competition with $\text{Ru}(\text{NH}_3)_6^{2+} \rightarrow \text{Ru}^{3+}$ charge recombination. Consequently, we also measured kinetics using the irreversible quencher $\text{Co}(\text{NH}_3)_5\text{Cl}^{2+}$; consistent results were obtained with the two quenchers. At the protein concentrations used in these experiments (5 to 40 μM), bimolecular $\text{Cu}^+ \rightarrow \text{Ru}^{3+}$ ET in the His^{126} derivative occurred on the same time scale as intramolecular $\text{Cu}^+ \rightarrow \text{Ru}^{3+}$ ET; the intramolecular ET rate was extracted from extrapolation of the observed ET rates to infinite dilution.
- T. B. Karpishin, M. W. Grinstaff, S. Komar-Panicucci, G. McLendon, H. B. Gray, *Structure* **2**, 415 (1994).
- We obtained all distances by molecular modeling, using the program Enzymix [F. S. Lee, Z. T. Chu, A. Warshel, *J. Comput. Chem.* **14**, 161 (1993)]. We obtained the final distance by averaging the distances in snapshots taken at 1-ps intervals during 200 ps of constrained dynamics simulation. In all cases, convergence was reached after approximately 20 to 30 ps of simulation.
- G. W. Canters and M. van de Kamp, *Curr. Opin. Struct. Biol.* **2**, 859 (1992); H. Nar, A. Messerschmidt, R. Huber, M. van de Kamp, G. W. Canters, *J. Mol. Biol.* **221**, 765 (1991); *FEBS Lett.* **306**, 119 (1992).
- The pathway model predicts that the coupling across space gaps drops off as an exponential function of distance (decay constant of 3.4 \AA^{-1}) (6). For the Cu-Met^{121} interaction, the gap is taken as the difference between the observed Cu-S separation and a covalent Cu-S bond distance ($\sim 2.3 \text{ \AA}$).
- M. D. Lowery and E. I. Solomon, *Inorg. Chim. Acta* **200**, 233 (1992).
- Many of the donor-acceptor systems examined by Dutton and co-workers (4) are part of the photosynthetic reaction center in which the redox sites are separated by α -helical secondary structures [H. Michel, J. Drenthofer, J. O. Epp, *EMBO J.* **5**, 2445 (1986)]. Donor-acceptor electronic coupling decays much more rapidly with distance in Ru-modified myoglobin, an α -helical dioxygen-binding protein, than in azurin or cyt c (8).
- We thank D. R. Casimiro, K. Warncke, J. J. Regan, and J. N. Onuchic for helpful comments. Supported by NIH and NSF.

17 January 1995; accepted 23 March 1995

Controlled Folding of Micrometer-Size Structures

Elisabeth Smela,* Olle Inganäs, Ingemar Lundström

Several types of microactuators have been fabricated, from simple paddles to self-assembling and -disassembling cubes. Conducting bilayers made of a layer of polymer and a layer of gold were used as hinges to connect rigid plates to each other and to a silicon substrate. The bending of the hinges was electrically controlled and reversible, allowing precise three-dimensional positioning of the plates. The structures were released from the substrate with a technique based on differential adhesion. This method, which avoids the use of a sacrificial layer and allows the actuators to pull themselves off the surface, may have general applications in micromachining. Possibilities include the manufacture of surfaces whose light reflection or chemical properties can be switched.

As the electronic properties of conjugated, or conducting, polymers are tuned from insulating to metallic, there are concomitant changes in volume: When electrons are donated to or removed from the polymer chains, compensating ionic species are inserted or extracted (1). The process can be controlled by the application of a small voltage if the polymer is in contact with an electrolyte. The amount of charge that can be stored is substantial: In fully doped polyheterocyclic polymers, approximately one dopant is incorporated for every four monomer units.

Conducting polymers compare favorably with piezoelectric materials, shape memory alloys, and magnetostrictive materials because they deliver high stresses, have substantial energy densities, and undergo large dimensional changes without requiring high voltages, currents, or temperatures for operation (2). Some potential applications of conducting polymers as electromechanical materials have been evaluated conceptually (3), and macroscopic bilayer actuators have been demonstrated (4, 5). Recently we produced micrometer-size bilayers (6), defining the geometrical elements photolithographically, and conducting polymer-polyimide cantilevers have been made (7).

The hinge or artificial muscle component of the devices described here is an

Linköping Institute of Technology, Department of Physics and Measurement Technology, S-581 83 Linköping, Sweden.

*To whom correspondence should be addressed.

application of these simple bilayers, which consist of a layer of conducting polymer, polypyrrole (PPy) doped with dodecylbenzenesulfonate (DBS), and a layer of gold. In this polymer system, the volume change is dominated by the simple physical separation of the chains due to cation insertion or extraction (8). The bilayer bends at a speed determined by the ionic species and the thickness of the polymer layer (because the volume change is controlled by diffusion). The extent to which the bilayer bends is determined by the thickness and elastic moduli of both layers. The sequence of photographs in Fig. 1 shows the extent to which the PPy-gold bilayers can reversibly curl, from flat strips to tight spirals. We used surface micromachining to fabricate these actuators (9).

By incorporating stiff parts into the structure, it is possible to considerably extend what can be accomplished with a basic bilayer. Figure 2 shows an array of paddles with surface dimensions of $90\ \mu\text{m}$ by $90\ \mu\text{m}$ rotating on hinges of $30\ \mu\text{m}$ by $30\ \mu\text{m}$. Note that these relatively short hinges produce a rotation of 180° . Hinges of that size were able to operate paddles as large as $900\ \mu\text{m}$ by $900\ \mu\text{m}$ but had difficulty initially releasing such large areas from the surface. Because only comparatively small hinges are needed to move large areas, it would be possible to design rigid flaps with different properties on either side: Activating the hinges would then transform virtually the entire surface. For an intuitive picture of the strength of these hinges, imagine a person under water trying with one arm to move a plate with dimensions of $30\ \text{m}$ by $30\ \text{m}$. It has been calculated that conducting polymers can deliver stresses of hundreds of megapascals (3), comparable to shape memory alloys.

Several rigid elements can be connected with bilayer hinges. Activation of the hinges causes the microstructure to fold and assemble into a predetermined shape. The device fabrication sequence for a center-mounted self-folding box with two consecutive hinges is illustrated and described in Fig. 3. The metal layers were deposited onto 3-inch silicon wafer substrates by vacuum evaporation and were patterned by wet chemical etching. The PPy was deposited electrochemically from an aqueous electrolyte containing Na^+DBS^- and pyrrole (10). The rigid benzocyclobutene (BCB) layer was deposited by spin-coating and cured at 200°C . Both polymer layers were patterned by reactive ion etching: PPy in an oxygen plasma and BCB in a mixture of 20% CF_4 in oxygen.

The key to the release of all of these microstructures is the weak adhesivity of selected areas of the surface produced in

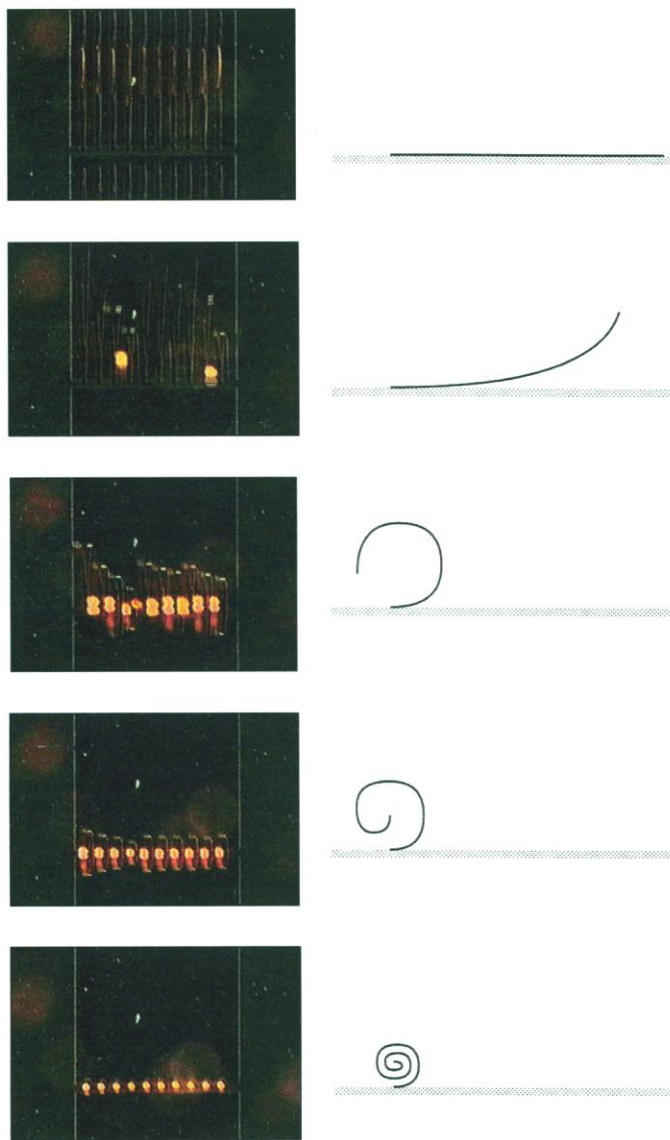


Fig. 1. Bilayer actuators, overhead view and adjacent schematic side view. Polypyrrole-gold bilayers with surface dimensions of $30\ \mu\text{m}$ by $1000\ \mu\text{m}$ in a liquid electrolyte curl into tight spirals in response to a change in the applied voltage from -1.0 to $+0.35\ \text{V}$ (top to bottom). The phenomenon is fully reversed upon return to $-1.0\ \text{V}$.

step A of Fig. 3. Rather than using sacrificial layers, which have to be removed in the final processing steps, we have developed an alternative release method based on differential adhesion in which the bilayer pulls parts of the completed device off the surface. Gold adheres weakly to bare silicon or silicon dioxide, so a thin layer (several angstroms) of a metal such as chromium, to which gold adheres well, is deposited first. However, because the gold film coheres to itself, a chromium layer with large holes can still hold down the entire film. The devices are positioned so that they are partly over the silicon and partly over the chromium. When they are operated, the tensile stress generated during the doping of the polymer pulls the gold free from the bare silicon, but the bilayers remain attached over the chromium. It is critical that the overlying rigid layer be almost stress-free, or the gold layer will be pulled off the silicon areas prematurely in step C of Fig. 3.

The differential adhesion method has several advantages. PPy does not need protection from chemical attack during a final etch release step, and arbitrarily large areas can be freed (it can take hours or days to etch a sacrificial layer out from underneath a large plate). Other methods and materials could be used to create the adhesion difference; for example, a patterned monolayer of silane molecules on silicon or a single material with areas of roughness and smoothness.

The devices were operated in a Na^+DBS^- electrolyte solution. A transparent indium tin oxide-coated glass plate was used as the counter electrode. The arrangement is illustrated in Fig. 4. Electrical contact to the devices was made through the chromium layer that remained over most of the surface. For structures that were center-mounted, like the boxes, the electrical path was completed through the conducting silicon wafer. In the present design, all of the bilayers were addressed simultaneously, but

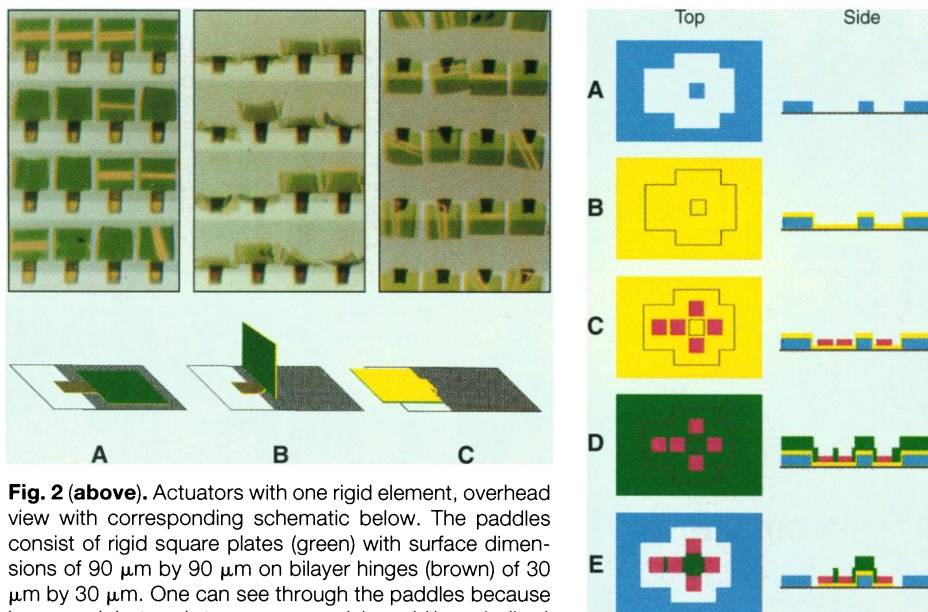


Fig. 2 (above). Actuators with one rigid element, overhead view with corresponding schematic below. The paddles consist of rigid square plates (green) with surface dimensions of $90\ \mu\text{m}$ by $90\ \mu\text{m}$ on bilayer hinges (brown) of $30\ \mu\text{m}$ by $30\ \mu\text{m}$. One can see through the paddles because benzocyclobutene is transparent and the gold layer (yellow) is very thin. **(A)** Paddles lie flat at 0° . **(B)** Paddles are perpendicular to the surface around 90° . **(C)** Paddles lie flat at 180° . The position of the paddles is controlled by the applied voltage. **Fig. 3 (right).** Processing sequence for self-opening and self-closing boxes. The figure is schematic and not to scale, and the vertical dimensions are greatly exaggerated. Only three masks were used. **(A)** A layer of chromium (blue) is evaporated onto a silicon wafer and patterned. **(B)** A gold film (yellow) is evaporated onto the surface. **(C)** A passive, rigid polymer, BCB, is deposited on the surface by spin-coating and is patterned (red). **(D)** PPy (green) is grown electrochemically onto the gold electrode. **(E)** The PPy and gold are patterned. Gold remains under the BCB and PPy, mechanically connecting them and providing electrical contact. When PPy is oxidized and reduced, its volume changes; the bilayers lift the plates from the silicon surface. The area in the center of the box remains attached to the surface by the chromium. The layer thicknesses are approximately $200\ \text{\AA}$ (gold), $5000\ \text{\AA}$ (BCB), and $3000\ \text{\AA}$ (PPy).

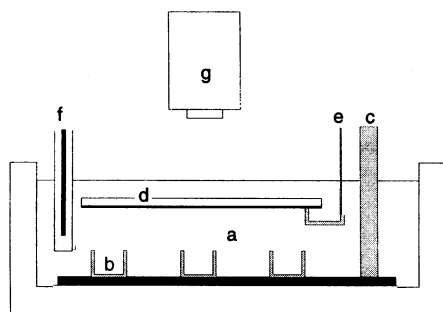


Fig. 4. Electrochemical cell. The devices were operated in a liquid electrolyte (a) in a polytetrafluoroethylene dish. Electrical contact to the devices (b) was made through a gold-plated screw (c) that also fixed the wafer in position. A transparent indium tin oxide-coated glass slide (d) served as the counter electrode and was contacted by a gold wire (e). The reference electrode (f) was Ag/AgCl. Pictures were taken through a microscope (g).

with the appropriate wiring it would be possible to address the different devices and the various hinges of a single device individually.

The PPy film after growth is always doped (contains no Na^+) and conducting, but the structures lie flat. During the first several oxidation-reduction cycles, however, the polymer chains undergo a per-

manent rearrangement so that in the doped state they take up less volume. From then on, when negative potentials are applied and the PPy film fills with Na^+ (the reduced or undoped state), it expands to its original size. When positive voltages are applied to the working electrode, the volume of the PPy layer contracts and the bilayer bends.

The potential between the devices and reference electrode was varied between -1.0 and $+0.35\ \text{V}$. Figure 5 shows a series of photographs of a center-mounted box closing around two small grains of sand. The plates can be held in any position by fixing the voltage to maintain a certain doping level. This permits one to do delicate manipulations or, with separately addressed plates, complex folding sequences. A three-hinge, side-mounted cube is shown closed in Fig. 6. These structures were able to change shape in 0.5 to 10 s, depending on the PPy thickness, when the voltage was changed abruptly between the two limits. The maximum current density for oxidation or reduction of a $4000\ \text{\AA}$ thick PPy film on gold is typically $10\ \text{mA}/\text{cm}^2$.

Bilayer cantilevers are a common feature in micromachined structures. However, conducting polymers undergo much larger volume changes than solid-state materials

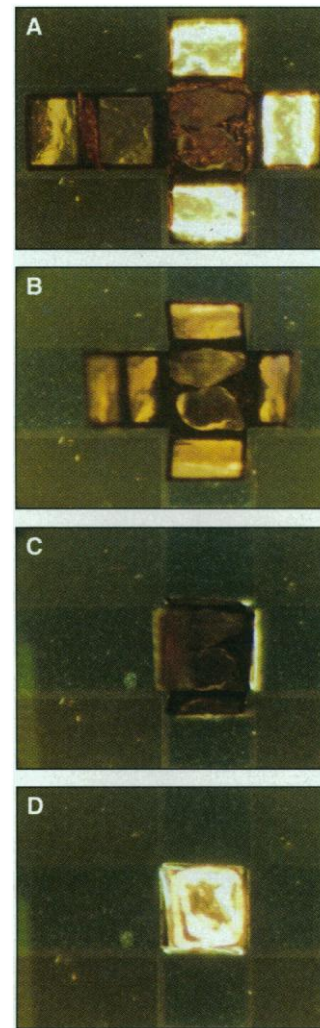


Fig. 5. Actuators with two consecutive rigid elements. This sequence of photographs shows a cubic box as it closes **(A to D)**. Each of the six sides is $300\ \mu\text{m}$ by $300\ \mu\text{m}$. Because BCB is transparent, the gold shines through the sides of the boxes. The two enclosed particles are small grains of sand. Folding from **(A)** to **(D)** took about 1 s.

such as piezoceramics or rare-earth magnetostrictive compounds, and smaller voltages and currents are required for operation (2). Bilayers made of two types of polyimide and driven by differences in coefficients of thermal expansion have been shown to have large displacements (11). However, the temperature in those actuators exceeds 250°C ; the room-temperature operation of conducting polymers would be more suitable for biological applications such as cell handling.

The combination of rigid and flexible micromachined elements is starting to attract interest. Electrostatically driven actuators consisting of rigid plates connected by elastic polyimide hinges have been made (12). In these devices, a polyimide film forms a flexible connection to the plates, which can be tilted up to 30° by

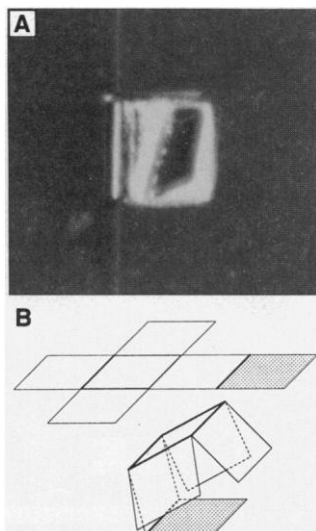


Fig. 6. Actuators with three consecutive rigid elements. **(A)** Photograph of a closed, side-mounted box with three consecutive hinges and the same dimensions as the cube in Fig. 5. **(B)** Schematic illustration.

applying several hundred volts between the plate and the substrate. The key difference between this approach and our approach is that we control the bending of the hinge rather than the position of the plate. The conducting polymer devices can therefore achieve folding of 180° at each joint.

Further applications of the described technology might include valves that close automatically in response to a chemical signal or a change in pH and structures for single-cell capture and analysis. More sophisticated folding structures could perhaps be used as microrobot limbs.

REFERENCES AND NOTES

1. R. B. Kaner and A. G. MacDiarmid, *Sci. Am.* **258**, 60 (February 1988); J. R. Reynolds, *Chemtech* (July 1988), p. 440; M. G. Kanatzidis, *Chem. Eng. News* (3 December 1990), p. 36; K. F. Schoch and H. E. Saunders, *IEEE Spectrum* **29**, 52 (June 1992); T. Studdt, *Res. Dev.* (October 1991), p. 94; W. R. Salaneck, I. Lundström, B. Rånby, Eds., *Conjugated Polymers and Related Materials: The Interconnection of Chemical and Electronic Structure* (Oxford Science Publications, Oxford, 1993); J. L. Brédas and R. Silbey, Eds., *Conjugated Polymers: The Novel Science and Technology of Highly Conducting and Nonlinear Optically Active Materials* (Kluwer, Dordrecht, Netherlands, 1991).
2. I. W. Hunter and S. Lafontaine, *IEEE Solid-State Sens. Actuator Workshop Tech. Dig.*, Hilton Head, SC, 22 to 25 June 1992, pp. 178–185.
3. R. H. Baughman, L. W. Shacklette, R. L. Eisenbaumer, E. J. Plichta, C. Becht, in *Molecular Electronics*, P. I. Lazarev, Ed. (Kluwer, Dordrecht, Netherlands, 1991), pp. 267–289.
4. Q. Pei and O. Inganäs, *Synth. Met.* **55–57**, 3730 (1993).
5. E. Smela, O. Inganäs, Q. Pei, I. Lundström, *Adv. Mat.* **5**, 630 (1993); "Physicists make tiny fingers for tiny jobs," *Science* **261**, 1119 (1993).
6. E. Smela, O. Inganäs, I. Lundström, in *Proceedings of the Electronics Biotechnology Advanced Forum*, Elba, Italy, 10 to 12 March 1994 (Plenum, New York,

- in press); *J. Micromech. Microeng.* **3**, 203 (1993).
7. A. P. Lee, K. C. Hong, J. Trevino, M. A. Northrup, in *Proceedings of the Dynamics Systems and Controls Division, Micro-Mechanical Systems Symposium of the International Mechanical Engineering Congress and Exposition*, Chicago, IL, 6 to 11 November 1994, C. J. Radcliffe, Ed. (American Society of Mechanical Engineers, New York, 1994), pp. 725–732.
 8. Q. Pei and O. Inganäs, *J. Phys. Chem.* **96**, 10507 (1992); *ibid.* **97**, 6034 (1993).
 9. For a review, see G. Delapierre, *Sens. Actuators* **17**, 123 (1989).
 10. Polypyrrole was chosen as the conducting polymer because it is fairly stable in aqueous solution and has good mechanical properties. It was electrochemically polymerized at a constant 0.6 V in a solution of 0.1 M pyrrole and 0.1 M sodium dodecylbenzenesulfonate (Na^+DBS^-) in deionized water. The evaporated gold film from step B in Fig. 3 served as the working electrode, a parallel gold-covered wafer was used as

a counter electrode, and an Ag/AgCl electrode provided the reference potential. DBS is a bulky anion that becomes immobilized in the polymer matrix during growth (7). Therefore, upon oxidation-reduction (doping-undoping), only cations (with their solvation shells) diffuse in and out of the polymer. Movement of both types of ionic species would be detrimental to the devices because it would complicate the behavior and cause long-term changes. The rigid-layer polymer BCB was obtained from Dow Chemical Corporation.

11. M. Ataka, A. Omodaka, N. Takeshima, H. Fujita, *J. Microelectromech. Syst.* **2**, 146 (1993).
12. K. Suzuki, I. Shimoyama, H. Miura, *ibid.* **3**, 4 (1994).
13. This work was supported by the Närings och Teknikutvecklings Verket, the Swedish Board for Industrial and Technical Development, through the Microelectronics program.

7 December 1994; accepted 7 April 1995

A Combinatorial Approach to Materials Discovery

X.-D. Xiang,* Xiaodong Sun, Gabriel Briceño, Yulin Lou, Kai-An Wang, Hauyee Chang, William G. Wallace-Freedman, Sung-Wei Chen, Peter G. Schultz*

A method that combines thin film deposition and physical masking techniques has been used for the parallel synthesis of spatially addressable libraries of solid-state materials. Arrays containing different combinations, stoichiometries, and deposition sequences of BaCO_3 , Bi_2O_3 , CaO , CuO , PbO , SrCO_3 , and Y_2O_3 were generated with a series of binary masks. The arrays were sintered and BiSrCaCuO and YBaCuO superconducting films were identified. Samples as small as 200 micrometers by 200 micrometers in size were generated, corresponding to library densities of 10,000 sites per square inch. The ability to generate and screen combinatorial libraries of solid-state compounds, when coupled with theory and empirical observations, may significantly increase the rate at which novel electronic, magnetic, and optical materials are discovered and theoretical predictions tested.

Currently, there is tremendous interest in materials such as high-temperature superconductors, supermagnetic alloys, metal oxide catalysts, and luminescent materials (1). However, few general principles have emerged that allow a priori prediction of the structures of new materials with enhanced properties (2). Consequently, the discovery of such materials remains a time-consuming and rather unpredictable trial-and-error process, made even more difficult by the increasing complexity of modern materials. Hence there is a need for a more efficient and systematic way to search through the largely unexplored universe of ternary, quaternary, and higher order solid-

state compounds in order to discover materials with novel electronic, optical, magnetic, or mechanical properties.

In biology, molecules with a desired property are often identified by the synthesis and screening of large collections, or libraries, of structures. Perhaps the best such example is that of the humoral immune system, which can generate and screen some 10^{12} antibody molecules to identify one that specifically recognizes and binds a foreign pathogen (3). One of the first applications of molecular libraries to chemistry was the development of catalytic antibodies (4). Shortly thereafter, a number of methods were developed for generating and screening large populations of biological molecules in vitro for binding, catalysis, or both (5, 6). A great deal of effort is currently devoted toward the application of these combinatorial libraries (libraries generated by combining large numbers of precursors), as well as libraries of small organic molecules (7), to the discovery of new drugs.

Here, we report the first application of the combinatorial approach to the discovery of new solid-state materials with novel

X.-D. Xiang, G. Briceño, K.-A. Wang, Molecular Design Institute, Lawrence Berkeley Laboratory, Berkeley, CA 94720, USA.

X. Sun, Y. Lou, H. Chang, W. G. Wallace-Freedman, S.-W. Chen, Department of Chemistry, University of California, Berkeley, CA 94720, USA.

P. G. Schultz, Molecular Design Institute, Lawrence Berkeley Laboratory, Berkeley, CA 94720, USA, and Department of Chemistry, University of California, Berkeley, CA 94720, USA.

*To whom correspondence should be addressed. World Wide Web URL: <http://www.inetbiz.com/matcomb>